Fast iterative sectional image reconstruction in optical scanning holography

Xin Zhang (1), Edmund Y. Lam (1) and T.-C. Poon (2)

1: Imaging Systems Laboratory, Department of Electrical and Electronic Engineering, The University of Hong Kong, Pokfulam Road, Hong Kong
2: Bradley Department of Electrical and Computer Engineering, Virginia Polytechnic Institute and State University, Blacksburg, Virginia 24061-0111
elam@eee.hku.hk

Abstract: Inverse imaging is a versatile technique for sectional image reconstruction in optical scanning holography. However, the matrix computation involved in the iterative process imposes a significant constraint on the size of the images. In this work, we develop a fast iterative method that circumvents the problem by taking advantage of the structures in the matrices. Experimental results show that we can handle large-size images about 64 times the previous size with a comparable amount of computation.

OCIS codes: (090.1760) Computer holography; (180.6900) Three-dimensional microscopy; (100.3190) Inverse problems; (100.3020) Image reconstruction-restoration; (110.1758) Computational imaging.

1. Introduction

The advantage of optical scanning holography (OSH) is that the entire three-dimensional (3D) volume of an object is recorded into a 2D hologram by lateral scanning [1]. Reconstruction methods have been proposed to obtain the sectional images in a hologram. Among them, the conventional method employs the complex conjugate impulse response to reconstruct sectional images. The Wiener filter [2] and the Wigner Distribution Function (WDF) [3] have also been used. But Wiener filter requires the noise spectrum, which is not observed during the acquisition of a hologram. Meanwhile, with the WDF, the huge computational burden and the interference terms known to exist with additive terms also limit the complexity of the hologram.

Analyzing the reconstruction as an inverse problem and conducting the reconstruction by inverse imaging is recently shown to be the most versatile, and it can handle more complicated holograms [4, 5]. However, the existing major limitation of this work is the significant computational load involved in the matrix multiplications. In this paper, we analyze the special structure of the matrices and improve the reconstruction by fast iterations to speed up the computation and allow for larger size images.

2. Imaging Model

Poon illustrated an OSH system and analyzed it in details [6]. Because OSH is a linear space-invariant system [7], we can use the convolution operation to describe a hologram. Furthermore, the convolution can be represented by a matrix multiplication. Suppose the hologram contains two sections at z_1 and z_2. We use a lexicographical ordering to convert sectional intensities at z_1 and z_2 into vectors and denote them as ψ_1 and ψ_2 respectively. Similarly, we convert the observed hologram, $g_c(x, y)$ into a vector and refer to it as γ_c. We then form two matrices, H_1 and H_2, using values from point spread functions at z_1 and z_2 respectively, so that a hologram is related in the form of matrices as [4]

$$\gamma_c = H_1\psi_1 + H_2\psi_2. \tag{1}$$

We take noise into account and simplify Eq. (1) further by writing

$$\gamma_c = H\psi + n, \tag{2}$$

where $H = \begin{bmatrix} H_1 & H_2 \end{bmatrix}$, $\psi = \begin{bmatrix} \psi_1^T & \psi_2^T \end{bmatrix}^T$ and n stands for the noise. Finding ψ from γ_c is therefore an inverse imaging problem. Note that this formulation can be extended for multiple sections.

3. Computational Considerations and Improvements

Because of the ill-posed nature of the inverse imaging problem, we can only find an approximation of ψ in the equation [8]. Regularization is employed to obtain the solution. We formulate the image reconstruction as an optimization problem [9], which seeks to minimize

$$f(\psi) = \| A\psi - \gamma_c \|^2 + \lambda \| C\psi \|^2, \text{ where } A = \begin{bmatrix} \mathrm{Re}[H_1] & \mathrm{Re}[H_2] \\ \mathrm{Im}[H_1] & \mathrm{Im}[H_2] \end{bmatrix}. \quad (3)$$

$\mathrm{Re}[\cdot]$ and $\mathrm{Im}[\cdot]$ means taking the real and imaginary parts, respectively. $\| \cdot \|$ denotes the L_2 norm, C stands for the Laplacian operator, and λ is the regularization parameter. We use the conjugate gradient (CG) method to solve the set of linear equations [10, 11].

Because both H_1 and H_2 are block-circulant-circulant-block (BCCB) matrices if we assume periodic extension on the boundary [12], we can convert it to an implementation using fast Fourier transform [13, 14]. We take an example to illustrate the technique. Suppose a BCCB matrix K_{mn} is an $m \times m$ block circulant matrix with $n \times n$ circulant blocks and a vector y is of length $m \times n$. That is,

$$K = \begin{bmatrix} K_1 & K_2 & \dots & K_m \\ K_m & K_1 & \dots & K_{m-1} \\ \vdots & \vdots & \ddots & \vdots \\ K_2 & K_3 & \dots & K_1 \end{bmatrix}, K_i = \begin{bmatrix} c_1 & c_2 & \dots & c_n \\ c_n & c_1 & \dots & c_{n-1} \\ \vdots & \vdots & \ddots & \vdots \\ c_2 & c_3 & \dots & c_1 \end{bmatrix}, \ y = \begin{bmatrix} a_1 \\ a_2 \\ \vdots \\ a_k \end{bmatrix}, \text{ and } k = m \times n. \quad (4)$$

The BCCB matrix-vector product Ky can be calculated as follows. Both y and the first column of the BCCB matrix K are arranged into $m \times n$ matrices, $Y^{(0)}$ and $K^{(0)}$. They are

$$Y^{(0)} = \begin{bmatrix} a_1 & a_2 & \dots & a_n \\ a_{n+1} & a_{n+2} & \dots & a_{2n} \\ \vdots & \vdots & \ddots & \vdots \\ a_{k-n+1} & a_{k-n+2} & \dots & a_k \end{bmatrix}, \text{ and } K^{(0)} = \begin{bmatrix} c_{1,(1)} & c_{n,(1)} & \dots & c_{2,(1)} \\ c_{1,(m)} & c_{n,(m)} & \dots & c_{2,(m)} \\ \vdots & \vdots & \ddots & \vdots \\ c_{1,(2)} & c_{n,(2)} & \dots & c_{2,(2)} \end{bmatrix}. \quad (5)$$

$c_{i,(j)}$ means the ith element of the first column of the jth block in K matrix. The convolution of $Y^{(0)}$ and $K^{(0)}$ is computed by the inverse Fourier transform of a multiplication in the Fourier domain. After stacking the resulting convolution matrix into a vector through row-by-row, the final vector will be equal to the product Ky.

We cannot directly use the above technique in Eq. (3), because the A matrix consists of H_1 and H_2 which are themselves BCCB, but A is not. However, we can still make use of it as follows. Since $\mathrm{Re}[H_1]$, $\mathrm{Im}[H_1]$, $\mathrm{Re}[H_2]$ and $\mathrm{Im}[H_2]$ matrices are BCCB, the matrix-vector product $\mathrm{Re}[H_1]\psi_1$ can be calculated by the method we describe above. We further note that A is a block matrix with four BCCB submatrices. Vectors ψ_1 and ψ_2 come from the real sectional images. The product of each submatrix with a vector can therefore be calculated in a similar manner. Since the calculation in the Fourier domain replaces the multiplication in the space domain, we do not need to render the huge matrices A and C. A moderate amount of memory is enough to store these matrices.

4. Results

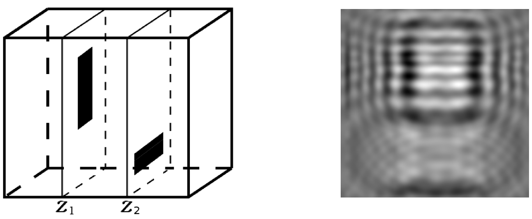

(a) The synthetic specimen (b) Sine hologram

Fig. 1. The specimen and hologram in the first experiment. Shown in Fig. 1(a) is the specimen, in which two elements are at z_1 and z_2 section, respectively. Shown in Fig. 1(b) is the sine hologram.

The experiment is performed on the synthetic specimen drawn in Fig. 1(a), which contains two elements in two distinct sections, $z_1 = 10\mathrm{mm}$ and $z_2 = 11\mathrm{mm}$, from the scanner of the OSH system. The two sections are scanned to generate a hologram by a HeNe laser. The size of sectional images in the specimen is 512×512, which is 64 times larger than our previous experiment reported in [4]. Optical scanning technique generates the complex hologram of

(a) (b)

Fig. 2. Reconstructed sections by the conventional method on the hologram containing two sections. Fig. 2(a) is the reconstructed result of z_1 section and Fig. 2(b) is that of z_2 section.

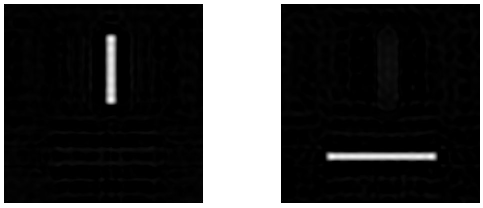

(a) (b)

Fig. 3. Reconstructed sections by the improved inverse imaging method from the hologram with two sections. Fig. 3(a) is reconstructed section at z_1 and Fig. 3(b) is the one at z_2.

the specimen. Fig. 1(b) presents the real part of the hologram (which is called the sine hologram [6]). Visually, it is hard to figure out any intensity distribution information of the two sections.

To obtain the sectional information from the complex hologram, reconstruction methods discussed above are implemented. The conventional method takes use of the convolution of the complex hologram with the conjugate impulse response at the focusing position to reconstruct the focused sectional image. Results by this method are shown in Fig. 2, in which Fig. 2(a) corresponds to the reconstructed section at z_1, and Fig. 2(b) to the one at z_2.

The inverse imaging method is also used on the specimen. The reconstructed images are shown in Fig. 3. As shown, each reconstructed section is hardly influenced by the defocus noise, and the element in each is clearly recovered. Signal-to-noise ratio (SNR) between the original sections and the recovered ones is 27.97 dB at z_1 and 27.12 dB at z_2. The time consumed in the reconstruction is 172 seconds and the number of iterations is 50. The experiment demonstrates that the reconstruction can recover sectional images without visible influence of defocus noise. Moreover, the use of features of BCCB matrix makes it possible to perform the reconstruction on a personal computer even when the size of the reconstructed sectional images is large.

5. Conclusions

OSH system is applicable to record the 3D volume information of an object, but requires computation to reconstruct the sectional images. Inverse imaging method is useful to achieve the reconstruction. We show that it is possible to avoid the storage of huge matrices and replace the matrix multiplication with the elementwise product in the Fourier domain making use of BCCB matrix.

Acknowledgment

This work was supported in part by the University Research Committee of the University of Hong Kong under Project 10208291.

References

1. B. D. Duncan and T.-C. Poon, “Gaussian Beam Analysis of Optical Scanning Holography,” J. Opt. Soc. Am. A **9**(2), 229–236 (1992).
2. T. Kim, “Optical Sectioning by Optical Scanning Holography and a Wiener Filter,” Applied Optics **45**(5), 872–879 (2006).
3. H. Kim, S.-W. Min, B. Lee, and T.-C. Poon, “Optical Sectioning for Optical Scanning Holography Using Phase-space Filtering with Wigner Distribution Functions,” Applied Optics **47**(19), 164–175 (2008).
4. X. Zhang, E. Y. Lam, and T.-C. Poon, “Reconstruction of sectional images in holography using inverse imaging,” Optics Express **16**(22), 17,215–17,226 (2008).
5. X. Zhang, T.-C. Poon, and E. Y. Lam, “An inverse imaging approach to sectional image reconstruction in optical scanning holography,” in *International Topical Meeting on Information Photonics* (2008).
6. T.-C. Poon, *Optical Scanning Holography with MATLAB*, 1st ed. (Springer-Verlag, New York, 2007).
7. G. Indebetouw, W. Zhong, and D. Chamberlin-Long, “Point-spread Function Synthesis in Scanning Holographic Microscopy,” J. Opt. Soc. Am. A **23**(7), 1708–1717 (2006).
8. J. M. Blackledge, *Digital Image Processing: Mathematical and Computational Methods*, 1st ed. (Horwood, West Sussex, 2005).
9. F. Natterer and F. Wübbeling, *Mathematical Methods in Image Reconstruction*, 1st ed. (SIAM, Philadelphia, 2001).
10. C. R. Vogel, *Computational Methods for Inverse Problems*, 1st ed. (SIAM, Philadelphia, 2002).
11. X. Zhang and E. Y. Lam, “Superresolution reconstruction using nonlinear gradient-based regularization,” Multidimens. Syst. Signal Process. pp. DOI: 10.1007/s11,045–008–0072–1 (2008).
12. M. R. Banham and A. K. Katsaggelos, “Digital Image Restoration,” IEEE Signal Processing Magazine **14**(2), 24–41 (1997).
13. M. K. Ng, *Iterative methods for Toeplitz systems*, 1st ed. (Oxford, Oxford, 2004).
14. R. H. Chan, *An introduction to iterative Toeplitz solvers*, 1st ed. (SIAM, Philadelphia, 2007).